

Self-Catenated and Interdigitated Layered Coordination Polymers Constructed from Kinked Dicarboxylate and Organodiimine Ligands

David P. Martin,[†] Ronald M. Supkowski,[‡] and Robert L. LaDuca^{*†}

Lyman Briggs College and Department of Chemistry, Michigan State University, East Lansing, Michigan 48825, and Department of Chemistry and Physics, King's College, Wilkes-Barre, Pennsylvania 18711

Received May 14, 2007

Hydrothermal combination of divalent nickel or cobalt nitrates with the kinked carboxylic acid 4,4'-oxybis(benzoic acid) (H₂oba) and the kinked and hydrogen-bonding capable organodiimine 4,4'-dipyridylamine (dpa) under basic conditions has afforded a pair of coordination polymers with a formulation of {[M(oba)(dpa)]·H₂O} (M = Ni, **1**; M = Co, **2**). Both materials were characterized by single-crystal X-ray diffraction, infrared spectroscopy, and thermogravimetric analysis. The structures of **1** and **2** are isomorphous and manifest intriguing self-catenated two-dimensional layered motifs with very rare non-diamond 6⁶ topology constructed from the direct covalent linkage of [M(oba)]_n double helices through [M(dpa)]_n undulating chains. Adjacent self-catenated layers engage in mutual interdigitation to form double-layer patterns that further aggregate via supramolecular hydrogen-bonding patterns imparted by the central amine of the dpa ligand. These coordination polymers are very thermally robust, with decomposition occurring only above 400 °C.

Introduction

Mutual entanglement of structural motifs is a very commonly encountered feature in coordination polymer chemistry.¹ Three-dimensional (3-D) coordination polymers can exhibit varying degrees of interpenetration, with higher numbers of distinct interpenetrated lattices promoted by long-spanning tethering ligands that maximize void spaces within a single covalently connected framework.² While many interpenetrated coordination polymers exhibit diamondoid (**dia**) frameworks because of the potential for large apertures, other 3-D structure types such as α-Po (**pcu**), cooperite (**pts**), and SrAl₂ (**sra**) can also display this behavior.³ However, self-catenated coordination polymers, where rods of the same framework penetrate through the shortest internodal circuits, are much rarer.^{4–10} Self-catenated materials can manifest

unique topologies, such as a (12,3)-topology chiral 3-D network in {[Ni(1,3,5-tri(4-pyridyl)triazine)(NO₃)₂]}⁴ and a rare 8-connected framework in [Cd₃(terephthalate)₃(L¹)₂(H₂O)₂] (L¹ = 1,4-bis(1,2,4-triazol-1-yl)butane).⁵ This intriguing genre of materials can also display potentially useful physical properties including photoluminescence⁶ and temperature-dependent spin crossover behavior.⁷

One of the best approaches toward the self-assembly and crystallization of self-penetrated/self-catenated coordination polymer networks involves the use of one or more conformationally flexible dipodal tethering ligands, usually dicarboxylates.^{8–10} The relatively short conformationally flexible succinate (suc) dianion has been one efficacious choice. {[Cd(suc)(L²)]·H₂O} (L² = *N,N'*-bispyridin-4-yl-methylsuccinamide) possesses [Cd(L²)] triple helices, linked

* To whom correspondence should be addressed. E-mail: laduca@msu.edu.

[†] Michigan State University.

[‡] King's College.

- (1) (a) Batten, S. R. *CrystEngComm* **2001**, *3*, 67–73. (b) Carlucci, L.; Ciani, G.; Proserpio, D. M. *Coord. Chem. Rev.* **2003**, *246*, 247–289.
- (2) Blatov, V. A.; Carlucci, L.; Ciani, G.; Proserpio, D. M. *CrystEngComm*, **2004**, *6*, 377–395.
- (3) Batten, S. R.; Robson, R. *Angew. Chem., Int. Ed.* **1998**, *37*, 1460–1494.
- (4) Abraham, B. F.; Batten, S. R.; Grannas, M. J.; Hamit, H.; Hoskins, B. F.; Robson, R. *Angew. Chem., Int. Ed.* **1999**, *38*, 1475–1477.

- (5) Wang, X.-L.; Qin, C.; Wang, E.-B.; Su, Z.-M. *Chem.—Eur. J.*, **2006**, *12*, 2680–2691.

- (6) Bi, M.; Li, G.; Zou, Y.; Shi, Z.; Feng, S. *Inorg. Chem.* **2007**, *46*, 604–606.

- (7) Niel, V.; Thompson, A. L.; Goeta, A. E.; Enachescu, C.; Hauser, A.; Galet, A.; Munoz, M. C.; Real, J. A. *Chem.—Eur. J.* **2005**, *11*, 2047–2060.

- (8) Lloyd, G. O.; Atwood, J. L.; Barbour, L. J. *Chem. Commun.* **2005**, 1845–1847.

- (9) Montney, M. R.; Mallika Krishnan, S.; Patel, N. M.; Supkowski, R. M.; LaDuca, R. L. *Crystal Growth Des.* **2007**, *7*, 1145–1153.

- (10) Wang, X. L.; Qin, C.; Wang, E.-B.; Li, Y.-G.; Su, Z.-M.; Xu, L.; Carlucci, L. *Angew. Chem., Int. Ed.* **2005**, *44*, 5824–5827.

into a very rare two-dimensional (2-D) self-penetrated sheet motif via tethering *gauche* conformation *suc* ligands.⁸ A unique self-penetrated 3-D 5-connected net with a uniform 6¹⁰ topology in {[Ni(dpa)₂(suc)_{0.5}]Cl} (dpa = 4,4'-dipyridylamine) was constructed by the linkage of quadruply interpenetrated [Ni(dpa)₂]_n²ⁿ⁺ adamantoid frameworks through *gauche* *suc* tethers.⁹ The longer kinked dicarboxylate ligand 4,4'-oxy(bisbenzoate) (oba) has also been used to promote the formation of polycatenated and self-penetrated coordination polymers. For instance, {[Ni(oba)(4,4'-bpy)]·2H₂O} exhibited a unique (3,5)-connected self-penetrated 3-D structure with (4.8²)(4.6⁴.8⁴.10) topology.¹⁰

This latter result and our own previous success in promoting self-penetration by means of the dpa ligand has inspired us to pursue mixed ligand coordination polymers with both oba and dpa tethers. These efforts have proven fruitful with the synthesis and crystallization of the isomorphous coordination polymers {[M(oba)(dpa)]·H₂O} (M = Ni, **1**; M = Co, **2**), which possess very rare 2-D self-catenated layers with an uncommon topology constructed from the junction of [M(oba)] double helices through dipodal dpa tethers.

Experimental Section

General Considerations. Metal nitrates were obtained commercially from Fisher and 4,4'-oxy(bisbenzoic acid) was purchased from Aldrich. 4,4'-dipyridylamine (dpa) was prepared via a published procedure.¹¹ Water was deionized above 3 MΩ in-house. Thermogravimetric analysis was performed on a TA Instruments TGA 2050 Thermogravimetric Analyzer with a heating rate of 10 °C min⁻¹ up to 600 °C. Elemental Analysis was carried out using a Perkin-Elmer 2400 Series II CHNS/O Analyzer. IR spectra were recorded on a Mattson Galaxy FTIR Series 3000 using KBr pellets.

Preparation of {[Ni(oba)(dpa)]·H₂O} (1**).** A mixture of Ni(NO₃)₂·6H₂O (81 mg, 0.28 mmol), 4,4'-oxy(bisbenzoic acid) (72 mg, 0.28 mmol), and dpa (95 mg, 0.56 mmol), along with 0.6 mL of a 1.0 M NaOH solution, was suspended in 10 g of H₂O (555 mmol) in a 23 mL Teflon-lined acid digestion bomb which was placed in a 120 °C oven for 48 h. The bomb was allowed to cool slowly to room temperature; then 93 mg (66% yield based on Ni) of green crystals of **1** were isolated after washing with distilled water, ethanol, and acetone and drying in air. Anal. Calcd for C₂₄H₁₉N₃NiO₆: C, 57.18; H, 3.80; N, 8.33%. Found: C, 57.47; H, 3.25; N, 8.43%. IR (KBr, ν, cm⁻¹): 3450 vw b, 3250 vw, 3150 vw, 3000 vw, 2900 vw, 1595 s, 1519 s, 1500 m, 1419 s, 1342 m, 1234 m, 1213 m, 1180 m, 1156 m, 1080 w, 1064 w, 1023 m, 903 w, 880 m, 849 m, 820 m, 781 m, 772 m, 724 m, 663 m.

Preparation of {[Co(oba)(dpa)]·H₂O} (2**).** Compound **2** was prepared in a manner similar to that for **1** except for the use of Co(NO₃)₂·6H₂O (81 mg, 0.28 mmol) as the metal precursor; 91 mg (65% yield based on Co) of **2** as magenta rhombs were isolated after washing with distilled water, ethanol, and acetone and drying in air. Anal. Calcd for C₂₄H₁₉CoN₃O₆: C, 57.15; H, 3.80; N, 8.33%. Found: C, 57.30; H, 3.16; N, 8.28%. IR (KBr, ν, cm⁻¹): 3450 vw b, 3250 vw, 3150 vw, 3000 vw, 2900 vw, 1595 s, 1519 s, 1500 m, 1419 s, 1342 m, 1234 m, 1213 m, 1180 m, 1156 m, 1080 w, 1064 w, 1023 m, 903 w, 880 m, 849 m, 820 m, 781 m, 772 m, 724 m, 663 m.

(11) Zapf, P. J.; LaDuca, R. L.; Rarig, R. S.; Johnson, K. M.; Zubieta, J. *Inorg. Chem.* **1998**, *37*, 3411–3414.

Table 1. Crystal and Structure Refinement Data for **1** and **2**

	1	2
empirical formula	C ₂₄ H ₁₉ N ₃ NiO ₆	C ₂₄ H ₁₉ CoN ₃ O ₆
fw	504.16	504.36
temp (K)	293(2)	293(2)
λ (Å)	0.71073	0.71073
cryst syst	monoclinic	monoclinic
space group	C2/c	C2/c
a (Å)	23.100(5)	22.849(7)
b (Å)	11.865(3)	11.832(4)
c (Å)	17.365(4)	17.514(6)
β (deg)	107.886(3)	108.324(5)
V (Å ³)	4529.3(17)	4495(2)
Z	8	8
D _{calcd} (g cm ⁻³)	1.473	1.485
μ (mm ⁻¹)	0.903	0.810
min/max T	0.823	0.849
<i>hkl</i> ranges	-30 ≤ <i>h</i> ≤ 29 -15 ≤ <i>k</i> ≤ 15 -22 ≤ <i>l</i> ≤ 21	-30 ≤ <i>h</i> ≤ 29 -15 ≤ <i>k</i> ≤ 15 -23 ≤ <i>l</i> ≤ 22
total reflns	23 750	24 772
unique reflns	5140	5216
R(int)	0.0237	0.0439
params/restraints	309/1	309/1
R ₁ ^a (all data)	0.0430	0.0693
R ₁ ^a (<i>I</i> > 2σ(<i>I</i>))	0.0351	0.0432
R ₂ ^b (all data)	0.0972	0.1148
R ₂ ^b (<i>I</i> > 2σ(<i>I</i>))	0.0931	0.1038
max/min residual (e ⁻ Å ⁻³)	0.449/-0.419	0.457/-0.304
GOF	1.066	1.044

$$^a R_1 = \sum ||F_o| - |F_c|| / \sum |F_o|. \quad ^b R_2 = \sum \{ [w(F_o^2 - F_c^2)]^2 / \sum [wF_o^2] \}^{1/2}.$$

X-ray Crystallography. A green rhomb of **1** (with dimensions 0.75 mm × 0.30 mm × 0.25 mm) and a magenta rhomb of **2** (with dimensions 0.65 mm × 0.30 mm × 0.25 mm) were subjected to single-crystal X-ray diffraction using a Bruker-AXS SMART 1k CCD instrument at 293(2) K. Reflection data were acquired using graphite-monochromated Mo Kα radiation (λ = 0.71073 Å). The data were integrated via SAINT.¹² Lorentz and polarization effect and multiscan absorption corrections were applied with SADABS.¹³ The structures were solved using direct methods and refined on F² using SHELXTL.¹⁴ All non-hydrogen atoms were refined anisotropically. Hydrogen atoms bound to carbon atoms were placed in calculated positions and refined isotropically with a riding model. The dpa amine hydrogen atoms in both materials were found via Fourier difference maps, then restrained at fixed positions and refined isotropically. The disordered water molecule positions in **1** and **2** were successfully modeled with partial occupancy ratios and were refined isotropically. Hydrogen atoms could not be found for the disordered water molecules. Relevant crystallographic data for **1** and **2** are listed in Table 1. Supramolecular contact information and incipient void space volumes were computed with PLATON software.¹⁵ Network topologies were calculated or verified using the OLEX¹⁶ and TOPOS¹⁷ software programs.

- (12) SAINT, *Software for Data Extraction and Reduction*, version 6.02; Bruker AXS, Inc.: Madison, WI, 2002.
- (13) SADABS, *Software for Empirical Absorption Correction*, version 2.03; Bruker AXS, Inc.: Madison, WI, 2002.
- (14) Sheldrick, G. M. *SHELXTL, Program for Crystal Structure Refinement*; University of Gottingen: Gottingen, Germany, 1997.
- (15) Spek, A. L. *PLATON, A Multipurpose Crystallographic Tool*; Utrecht University: Utrecht, The Netherlands, 1998.
- (16) Dolomanov, O. V.; Blake, A. J.; Champness, N. R.; Schroder, M. J. *Appl. Crystallogr.* **2003**, *36*, 1283.
- (17) Blatov, V. A.; Shevchenko, A. P.; Serezhkin, V. N. *J. Appl. Crystallogr.* **2000**, *33*, 1193.

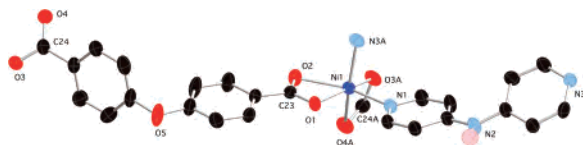


Figure 1. Expanded asymmetric unit of **1** with thermal ellipsoids at 50% probability and partial atom numbering scheme, showing complete coordination at Ni. Most hydrogen atoms and the disordered water molecules of crystallization are omitted. The asymmetric unit of compound **2** is very similar.

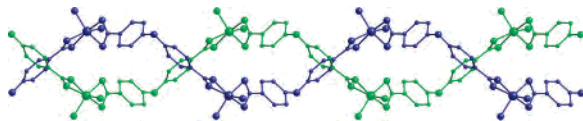


Figure 2. $[\text{Ni}(\text{oba})]_n$ double helix substructure in **1**.

Results and Discussion

Synthesis and Infrared Spectra. Hydrothermal combination of divalent cobalt or nickel nitrate with 4,4'-oxy-bis-(benzoic acid) (H_2oba) and 4,4'-dipyridylamine (dpa) with addition of base afforded single crystals of $\{[\text{M}(\text{oba})(\text{dpa})\cdot\text{H}_2\text{O}]\}$ ($\text{M} = \text{Ni}$, **1**; $\text{M} = \text{Co}$, **2**) cleanly and in high yield. While running these reactions at lower pH afforded microcrystalline **1** and **2** (according to powder XRD), basic conditions are required for large single crystals. The infrared spectra of compounds **1** and **2** were consistent with their formulations. Features corresponding to pyridyl ring puckering mechanisms were observed in the region between 600 and 820 cm^{-1} . Sharp, medium intensity bands observed in the range of ~ 1520 to ~ 1200 cm^{-1} arise from stretching modes of the pyridyl rings of the dpa moieties. Asymmetric and symmetric carboxylate stretching modes were observed at 1595 and 1419 cm^{-1} , respectively. The $\Delta\nu$ value of 176 cm^{-1} is indicative of the bisbridging bischelating binding mode of the oba ligands.¹⁸ Bands between 3050 and 3150 cm^{-1} represent C–H stretching modes. A broad band at ~ 3400 cm^{-1} represents the N–H subunit within the dpa ligands, overlapping with O–H stretching modes within the water molecules of crystallization. The broadness of these latter spectral features can be ascribed to the presence of hydrogen-bonding pathways (vide infra).

Structural Description of $\{[\text{M}(\text{oba})(\text{dpa})\cdot\text{H}_2\text{O}]\}$ -Coordination Polymers ($\text{M} = \text{Ni}$, **1; $\text{M} = \text{Co}$, **2**).** The asymmetric units of **1** and **2** were virtually identical, with both materials crystallizing in the centrosymmetric monoclinic space group $C2/c$. Both contain one divalent metal atom, one dianionic oba ligand, and one dpa ligand, along with one water molecule of crystallization disordered equally over two positions. (Elemental analysis and thermogravimetric analysis also indicated the presence of unligated water molecules.) The $\{\text{MO}_4\text{N}_2\}$ coordination spheres are each defined by two chelating oba carboxylate termini, with two *cis*-oriented dpa nitrogen donors. Bond lengths and angles about the metal centers in **1** and **2** are consistent with

Table 2. Selected Bond Distance (\AA) and Angle (deg) Data for **1** and **2**^a

1		2	
Ni1–N1	2.0453(17)	Co1–N1	2.074(2)
Ni1–N3 ^{#1}	2.0557(17)	Co1–N3 ^{#1}	2.100(2)
Ni1–O1	2.0658(14)	Co1–O1	2.338(2)
Ni1–O3 ^{#2}	2.0798(15)	Co1–O2	2.071(2)
Ni1–O4 ^{#2}	2.1887(16)	Co1–O3 ^{#3}	2.2889(19)
Ni1–O2	2.1890(15)	Co1–O4 ^{#3}	2.0861(17)
O1–C23	1.258(2)	O1–C23	1.243(3)
O2–C23	1.265(2)	O2–C23	1.249(4)
O3–C24	1.271(2)	O3–C24	1.260(3)
O4–C24	1.248(3)	O4–C24	1.263(3)
N1–Ni1–N3 ^{#1}	91.11(7)	O2–Co1–N1	112.69(9)
N1–Ni1–O1	94.60(6)	O2–Co1–O4 ^{#3}	110.57(8)
N3 ^{#1} –Ni1–O1	97.06(6)	N1–Co1–O4 ^{#3}	96.33(7)
N1–Ni1–O3 ^{#2}	96.43(7)	O2–Co1–N3 ^{#1}	135.80(8)
N3 ^{#1} –Ni1–O3 ^{#2}	94.47(6)	N1–Co1–N3 ^{#1}	93.18(8)
O1–Ni1–O3 ^{#2}	163.86(6)	O4–Co1–N3 ^{#1}	100.85(8)
N1–Ni1–O4 ^{#2}	99.57(7)	O2–Co1–O3 ^{#3}	84.13(8)
N3 ^{#1} –Ni1–O4 ^{#2}	154.59(7)	N1–Co1–O3 ^{#3}	155.00(7)
O1–Ni1–O4 ^{#2}	104.90(6)	O4–Co1–O3 ^{#3}	59.49(6)
O3 ^{#2} –Ni1–O4 ^{#2}	61.62(6)	N3 ^{#1} –Co1–O3 ^{#3}	86.02(8)
N1–Ni1–O2	156.12(6)	O2–Co1–O1	58.69(8)
N3 ^{#1} –Ni1–O2	91.90(7)	N1–Co1–O1	90.06(8)
O1–Ni1–O2	61.52(5)	O4 ^{#3} –Co1–O1	169.13(7)
O3 ^{#2} –Ni1–O2	106.93(6)	N3 ^{#1} –Co1–O1	87.52(8)
O4 ^{#2} –Ni1–O2	87.56(7)	O3 ^{#3} –Co1–O1	114.84(8)
C14–O5–C20	117.63(17)	C20–O5–C14	117.3(2)
C3–N2–C8	127.55(18)	C3–N2–C8	126.8(2)

^a Symmetry equivalent atoms: #1 $-x + 1/2, y + 1/2, -z - 1/2$; #2 $-x + 1, y - 1, -z + 1/2$; #3 $-x + 1, y + 1, -z + 1/2$.

distorted octahedral geometry caused by the presence of two chelating ligands and are given in Table 2. The largest *trans*-L–M–L bond angles in both cases are marked by oxygen donors from carboxylate termini from two different oba ligands. The Ni–O bond lengths in **1** vary only by ~ 0.01 \AA within each type of chelating carboxylate; the corresponding arrangement in **2** is much less symmetric, with Co–O bond lengths spanning a range from ~ 0.2 to ~ 0.3 \AA . In general, the bond lengths in **1** are shorter than those in **2**, consistent with well-known ionic radius trends.¹⁹ The inter-ring four-carbon-atom torsion angles within the dpa ligands in **1** and **2** are ~ 37.5 and $\sim 41.3^\circ$, respectively. Nevertheless, the gross structural features of **1** and **2** are largely similar despite the differences in their metrical parameters (vide infra).

Extension of the structures of **1** and **2** through the bisbridging, bischelating oba ligands reveals the presence of neutral $[\text{M}(\text{oba})]_n$ one-dimensional (1-D) double helices coursing parallel to the *b* crystal direction (Figure 2, shown for **1**). The helical substructure of a single metal dicarboxylate strand is likely imparted by the central ether kink within the oba ligands, which displays an inter-ring twist of $\sim 78^\circ$ in both **1** and **2**. The Ni–Ni contact distance through the oba tether in **1** is 14.389 \AA ; because of the longer bond lengths in **2**, the corresponding Co–Co distance is slightly extended, at 14.428 \AA . To accommodate the asymmetric chelating binding modes and longer Co–O bond lengths in **2**, the two carboxylate groups are twisted relative to their respective benzene rings by ~ 1 and $\sim 23^\circ$. The carboxylate groups within the oba ligands in **1** are twisted to a greater

(18) Nakamoto, K. *Infra-red Spectra of Inorganic and Co-ordination Compounds*; John Wiley and Sons: New York, 1963.

(19) Shannon, R. D. *Acta Crystallogr.* **1976**, *A32*, 751.

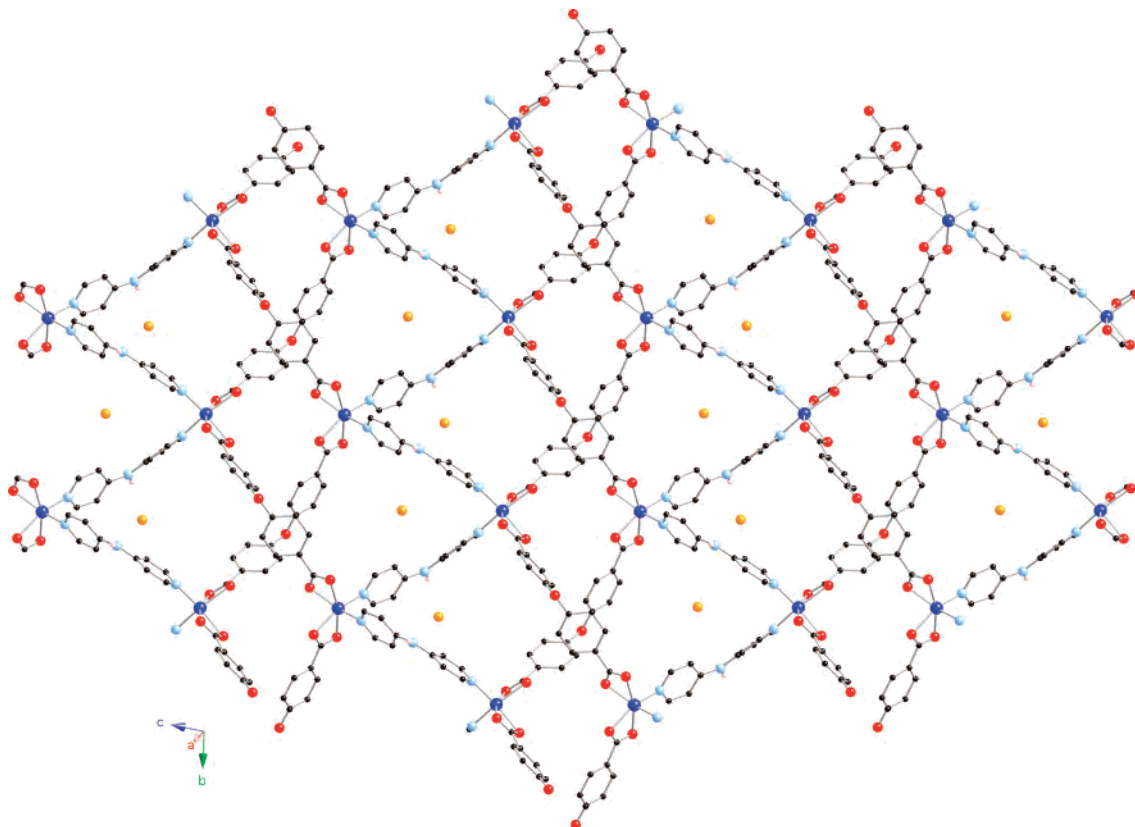


Figure 3. View down the *a* crystal axis of the self-catenated two-dimensional $[\text{Ni}(\text{oba})(\text{dpa})]$ layered motif in **1**. The oba ligands weave above and below the plane of the layer. Water molecules of crystallization are shown in orange.

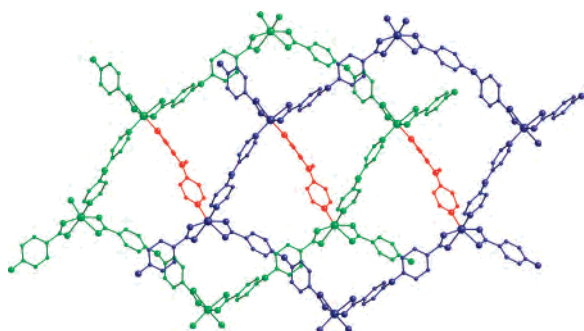


Figure 4. Magnified perspective of the self-catenation of two adjacent six-node circuits within a layer in **1**.

extent (~ 5 and $\sim 39^\circ$ torsions) in response to their more symmetric binding and slightly shorter Ni–Ni distance. The closest M–M distances between individual helices are 8.140 (in **1**) and 8.254 Å (in **2**).

Each $[\text{M}(\text{oba})]_n$ double helix is then joined to two others through exobidentate dpa ligands to construct a 2-D layer motif resting parallel to the *bc* crystal plane (Figure 3). The M–M contact distances through the dpa ligands measure 11.216 (**1**) and 11.136 Å (**2**), with a similar inverse trend between dpa torsion angle and metal–metal contact distance as in prior succinate-based coordination polymers.⁹ Each metal atom therefore serves as a 4-connected node. Two of these connections occur through oba ligands within a single helical strand, which weave over and under each other and project above and below the plane of the layer. The dpa ligands then permit conjunction to two other metal atoms,

each belonging to a different strand within an adjacent double helical motif. Thus, each single strand is connected to both strands in an adjacent double helix. As a result the structures of **1** and **2** are composed of self-catenated layers with a very rare non-diamond 6^6 topology, with a long vertex symbol of $6_2 \cdot 6_2 \cdot 6_3 \cdot 6_6 \cdot 6_4 \cdot 6_4$ as determined by TOPOS. Feng and co-workers have recently prepared a self-penetrated coordination polymer, $[\text{Cu}_4\text{I}_4(\text{DABCO})_4]$, that possesses a non-diamond 6^6 topology.⁶ However, Feng's material has three-dimensional covalent connectivity; to the best of our knowledge, **1** and **2** are the first examples of a *two-dimensional* 6^6 coordination polymer topology.

A magnified view of the intralayer self-catenation is presented in Figure 4, in which individual interwoven $(\text{M}-\text{oba}-\text{M}-\text{oba}-\text{M}-\text{dpa})_2$ 6-node circuits (in green and blue) are joined by the dpa ligands outlined in red. The longest through-space contact distances across a single 6-node circuit in **1** are 20.183 (Ni–Ni) and 25.070 Å ($\text{O}_{\text{ether}}-\text{O}_{\text{ether}}$); the corresponding distances in **2** are 20.100 and 25.059 Å. Water molecules of crystallization lie within incipient void spaces inside the layers, held loosely by weak C–H \cdots O hydrogen-bonding pathways provided by the dpa ligands (C \cdots O distances = ~ 3.05 – 3.15 Å). The solvent-bearing void volumes are comparable in both cases, occupying 7.9 (**1**) and 8.1% (**2**) of the respective unit cell volumes.

Abutting self-catenated $[\text{M}(\text{oba})(\text{dpa})]$ layers interdigitate with each other, stacking along the *a* crystal direction to establish the *pseudo*-3-D structures of **1** and **2** (Figure 5).

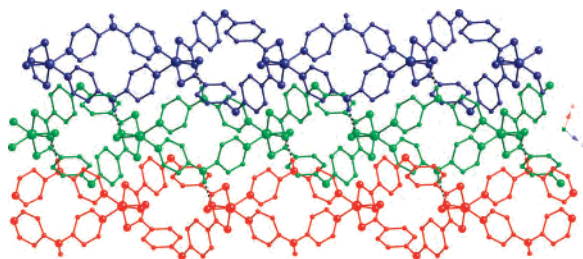


Figure 5. Interdigitation of self-penetrated $[\text{Ni}(\text{oba})(\text{dpa})]_n$ layers in **1**. Interlayer hydrogen bonding between dpa central amine units and ligated carboxylate oxygen atoms is shown as dashed lines.

Table 3. Interlayer Hydrogen-Bonding Distance (Å) and Angle (deg) Data for **1** and **2**

	D–H	$d(\text{H}\cdots\text{A})$	$\angle\text{DHA}$	$d(\text{D}\cdots\text{A})$	symmetry transformation for A
1	N2–H2N \cdots O2	1.93(2)	171(2)	2.761(3)	$x, -y + 1, z - 1/2$
2	N2–H2N \cdots O3	1.86(3)	170(3)	2.739(5)	$-x + 1, -y - 1, -z$

The interdigitation is promoted by hydrogen-bonding between dpa amine N–H groups in one layer and a ligated carboxylate oxygen atoms in the next. Geometric parameters for these supramolecular interactions are given in Table 3. Interlayer aggregation is supplemented by relatively strong π – π stacking (3.720(2) Å, as calculated by PLATON) between dpa pyridyl rings and oba benzene rings in juxtaposed layers. The interdigitation allows relatively tight packing of the layers, causing nearest-neighbor interlayer M–M contact distances of ~ 5.5 Å, substantially closer than any intralayer M–M interaction. Neighboring layers are related by crystallographic inversion centers. Therefore the helices within these layers are of opposite handedness, eliminating the possibility of acentricity.

A comparison of the structures of **1** and **2** with other divalent metal oba/organodiimine coordination polymers reveals the importance of both the kinked oba and dpa ligands in the promotion of the observed unique 2-D self-catenated morphologies. Employment of the flexible tethering diimine 1,2-di-4-pyridylethane (bpe) resulted in $\{[\text{Ni}(\text{oba})(\text{bpe})\cdot\text{H}_2\text{O}]\}$ and $[\text{Co}(\text{oba})(\text{bpe})]$, which displayed interpenetrated but “standard” 2-D (4,4) rhomboid grid coordination polymer layers.²⁰ An attempt to prepare a similar cadmium derivative afforded the one-dimensional coordination polymer $[\text{Cd}(\text{Hoba})_2(\text{bpe})]$.²¹ In these oba/bpe cases, the nitrogen donors of the bpe ligands are disposed in a *trans* manner at the respective metal atoms. It is plausible that the *cis* disposition of the dpa nitrogen donors in **1** and **2** promotes a zigzag $[\text{Ni}(\text{dpa})]$ chain-type motif that allows conjunction of the $[\text{Ni}(\text{oba})]$ double helices into the observed self-catenated layer pattern. Although a *cis* arrangement of the organodiimine ligands exists in $\{[\text{Ni}_2(\text{oba})_2(4,4'\text{-bpy})_2(\text{H}_2\text{O})_2]\cdot 4,4'\text{-bpy}\}$,²⁰ 1d \rightarrow 2D polycatenation of “trainlike” box motifs is observed instead of interpenetration. It is most likely that the two kinked ligands, by imposition of a unique covalent and supramolecular environment, act in tandem to instigate formation of the novel structures of **1** and **2**.

Thermogravimetric Analysis and Dehydration Behavior. Compound **1** underwent slow dehydration between ambient temperature and ~ 410 °C (4.2% mass loss observed, 3.6% predicted for 1 equiv of water), upon which decomposition commenced. A mass loss of 66.0% corresponding to the loss of one equivalent of oba and a pyridine fragment was complete by ~ 480 °C (66.9% predicted for the combined mass loss). A further mass loss denotes the combustion or expulsion of the remaining organic components. The final remnant at ~ 895 °C of 11.7% of the original mass corresponds to the deposition of Ni metal (11.6% calcd). To probe the structural integrity of **1**, a sample was heated at 180 °C for 24 h. Powder XRD indicated that the self-catenated layered coordination polymer stayed intact. Compound **2** also dehydrated slowly between 25 and ~ 410 °C (3.8% mass loss, 3.6% predicted for 1 equiv of water), at which point, expulsion of the organic ligands occurred. A decrease in mass corresponding to the loss of one equivalent of oba was complete by ~ 510 °C (49.4% mass loss observed, 51.2% predicted). This was followed by a mass loss of 34.5% between this temperature and ~ 825 °C corresponding to the removal of 1 equiv of dpa (33.9% mass loss predicted). The remaining 12.5% of the original mass corresponds to residual Co metal (11.6% predicted).

Conclusion

Employment of the kinked ligands 4,4'-oxy(bisbenzoate) and 4,4'-dipyridylamine has permitted hydrothermal synthesis of two isomorphous coordination polymers with a very uncommon non-diamond 6⁶ topology, which represent two new entries in the extremely small list of 2-D self-catenated layered structures.^{8,22,23} Synergistic interactions between covalent bonding modes imparted by the kinked donor dispositions of the mixed ligand system and supramolecular hydrogen bonding and π – π stacking mechanisms in turn promote interdigitation and aggregation of neighboring layers. In addition, the self-catenated morphology provides incipient voids within the coordination polymer matrices and imputes a high degree of thermal stability. While substantially more experimental work will be required to gain the ability to deliberately design particular self-penetrated frameworks, judicious variance of the conformational flexibility and donor disposition of long flexible or kinked tethering ligands is likely to advance this intriguing aspect of coordination polymer structural chemistry.

Acknowledgment. The authors gratefully acknowledge Michigan State University for financial support of this work. The thermogravimetric analyzer at King's College was purchased with a grant from the Alden Trust. We thank Dr. Rui Huang (MSU) for elemental analysis and Lindsey Johnston for acquiring the infrared spectra.

Supporting Information Available: TGA traces for **1** and **2** (Figures S1 and S2) and the powder XRD spectrum after heat

(20) Sun, C.-Y.; Zheng, X.-J.; Gao, S.; Li, L.-C.; Jin, L.-P. *Eur. J. Inorg. Chem.* **2005**, 4150–4159.

(21) Yin, D.-W.; Xiao, H.-P. *Acta Crystallogr.* **2005**, E61, m708–m710.

(22) Carlucci, L.; Ciani, C.; Macchi, P.; Proserpio, D. M.; Rizzato, S. *Chem.–Eur. J.* **1999**, 5, 237–243.

(23) Rizk, A. T.; Kilner, C. A.; Halcrow, M. A. *CrystEngComm* **2005**, 7, 359–362.

treatment of **1** (Figure S3). This material is available free of charge via the Internet at <http://pubs.acs.org>. Crystallographic data in CIF format for **1** and **2** have been deposited with the Cambridge Crystallographic Data Centre with nos. 642623 and 642624, respectively. Copies of the data can be obtained free of charge via

the Internet at <http://www.ccdc.cam.ac.uk/conts/retrieving.html> or by post at CCDC, 12 Union Road, Cambridge CB2 1EZ, U.K. (fax: 44–1223336033; e-mail: deposit@ccdc.cam.ac.uk).

IC700931U